

Accepted Manuscript

Early diagnosis of Zika infection using a ZnO nanostructures-based rapid electrochemical biosensor

Aline Macedo Faria, Talita Mazon



PII: S0039-9140(19)30478-3

DOI: <https://doi.org/10.1016/j.talanta.2019.04.080>

Reference: TAL 19879

To appear in: *Talanta*

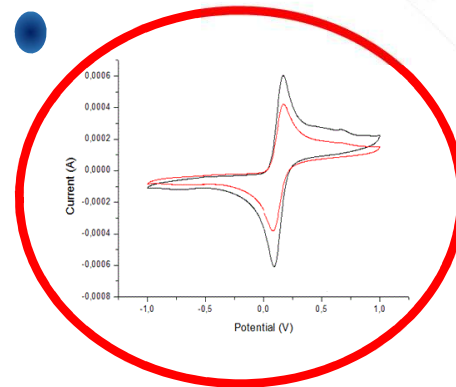
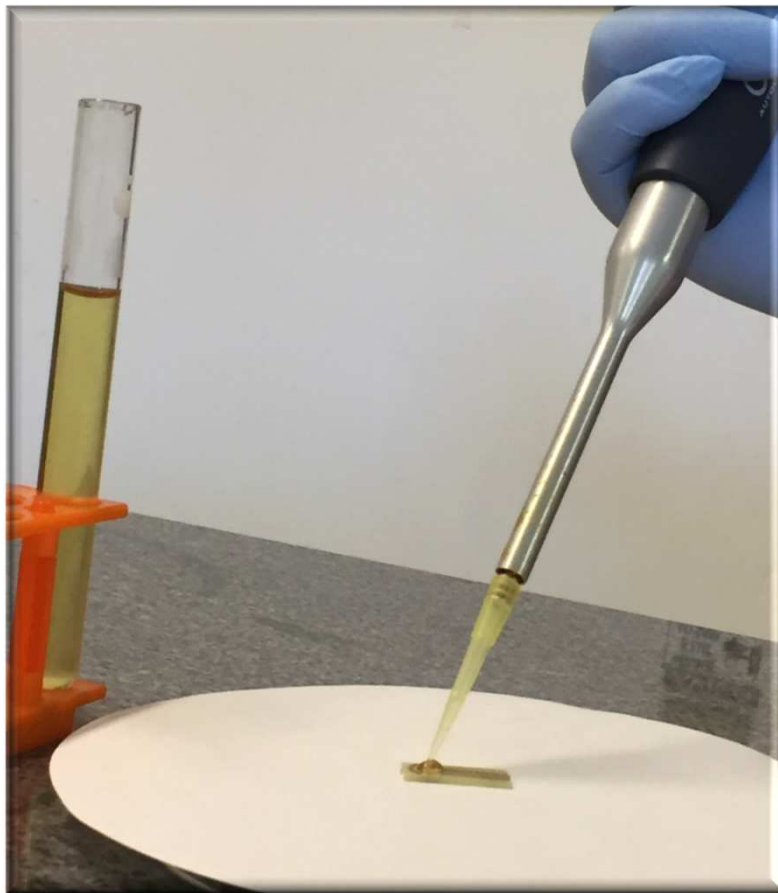
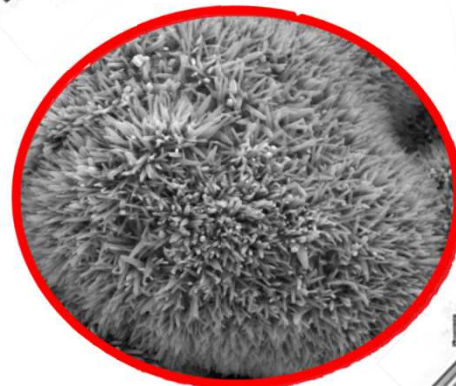
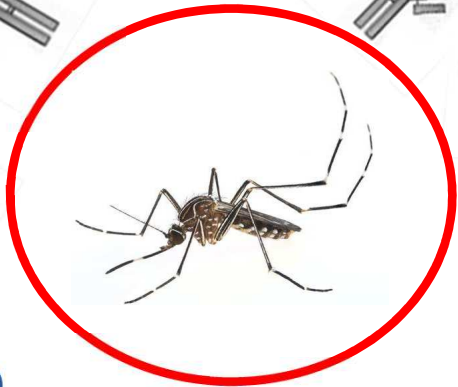
Received Date: 10 January 2019

Revised Date: 7 April 2019

Accepted Date: 28 April 2019

Please cite this article as: A.M. Faria, T. Mazon, Early diagnosis of Zika infection using a ZnO nanostructures-based rapid electrochemical biosensor, *Talanta* (2019), doi: <https://doi.org/10.1016/j.talanta.2019.04.080>.

This is a PDF file of an unedited manuscript that has been accepted for publication. As a service to our customers we are providing this early version of the manuscript. The manuscript will undergo copyediting, typesetting, and review of the resulting proof before it is published in its final form. Please note that during the production process errors may be discovered which could affect the content, and all legal disclaimers that apply to the journal pertain.



1 **Early Diagnosis of Zika Infection Using a ZnO Nanostructures-based Rapid**
2 **Electrochemical Biosensor**

3

4

Aline Macedo Faria, Talita Mazon*

5

6Centro de Tecnologia da Informação Renato Archer, CTI, Rod. D. Pedro I, KM 143.6,
713069-901, Campinas, SP, Brazil

8* Corresponding author: e-mail: talita.mazon@cti.gov.br; Centro de Tecnologia da

9Informação Renato Archer, CTI, Rod. D. Pedro I, KM 143.6, 13069-901, Campinas, SP,

10Brazil; Phone Number (+55) 19 3746-6185

11

12

13

14

15

16

17

18

19

20

21

22

23

24

25

26

27

28

29

30

31

32

33

34

35

36ABSTRACT

37

38In this work, we report a develop of electrochemical immunosensor based on ZnO
39nanostructures immobilized with ZIKV-NS1 antibody on Printed Circuit Board (PCB).
40ZnO nanostructures were grown on PCB by chemical bath deposition (CDB) and
41characterized by SEM. ZIKV-NS1 antibody was immobilized on the ZnO nanostructures
42surface via cystamine and glutaraldehyde. The samples were characterized by
43Immunofluorescence Confocal Microscopy and FTIR to identify the immobilization of the
44antibody to the sensor board. The analytical responses of the immunosensor were
45evaluated by Cyclic Voltammetry (CV). The biosensor developed here allows rapid
46detection of Zika virus in undiluted urine, without cross reactive with DENV-NS1 antigen,
47with linear range 0.1ng mL^{-1} to 100 ng mL^{-1} . The limit of detection is lower than 1.00
48 pg.mL^{-1} . The biosensor is portable, cost-effectiveness, and simple to use, which makes it
49ideal for point-of-care applications.

50

51Keywords: Immunosensor; ZnO; Zika virus; dengue.

52

53

541. Introduction

55

56Zika virus (ZIKV) is a member of family *Flaviviridae* transmitted through the bite of
57infected *Aedes aegypti* mosquito. People with ZIKV disease can have symptoms, including
58headaches, mild fever, arthralgia, myalgia, rash and conjunctivitis [1]. Differential
59diagnosis based on ZIKV symptoms is still challenging once their often overlap with
60Dengue, Chikungunya and Yellow Fever [2]. Although zika fever is mostly asymptomatic,
61direct correlation between ZIKV infection in pregnant women and brain defect in fetuses is
62a major concern [3]. Because of this, the development of ZIKV diagnostic reliable tests is a
63crucial issue extensively studied nowadays. The diagnosis of ZIKV normally has two
64approaches developed for detecting it. One is based on sequencing of viral genomes, and
65other is detection of IgM and IgG produced by patients in response to exposure to ZIKV
66[4].

67RNA viral identified by genomic amplification (RT-PCR) [5,6], Elisa [7], CRISPR-Cas13
68[8], reverse-transcription loop-mediated amplification (RT-LAMP) [9],
69immunochromatography [10], Plaque Reduction Neutralization Test [11], assays are

70recommended for detecting ZIKV infection with high sensibility and selectivity. However,
71specificity in most ZIKV diagnosis is difficult to get due to cross reactive with Dengue
72virus. Besides, these techniques are expensive, take long time and require equipment and
73highly trained employees [12]. Considering the higher incidence of ZIKV infection is
74located in incoming countries, a specific, selective and sensible low-cost point-of-care test
75is needed.

76Electrochemical biosensor technology has been considered promissory for point-of-care
77(POC) device [13]. In this technology, the material used as working electrode, and the
78molecules used as bioreceptors, are critical parameters to ensure a low limit of detection,
79high selectivity and specificity [14, 15]. Nanomaterials-based working electrode is a
80promise by affording low limits of detection and better selectivity than traditional assays
81[16, 17]. Among the promise nanomaterials, zinc oxide nanorods (ZnO NRs) are easily
82synthesized with different morphologies and large specific area [18,19]. As a
83semiconductor with high chemical stability, ZnO NRs provide a suitable surface for
84immobilizing antibodies and an ideal path for effective carrier transport [20]. We have recently
85demonstrated use of ZnO NRs-based working electrodes as a sensitive, and cost-effective working
86electrode [21].

87With regard to bioreceptors, the use of Monoclonal antibodies makes biosensors more
88selective [22]. The non-structural protein 1 is an important molecule of the viruses in the
89flavivirus group, including Zika virus and Dengue [23 - 25]. Recent studies have shown
90that ZIKV-NS1 protein conformation has unique characteristics when compared to NS1
91proteins from other flaviviruses [12, 23]. This suggest NS1 may be a potential target for
92the diagnosis selective of Zika infection without cross reactive with another flavivirus.
93ZIKV-NS1 protein can be detected in urine thus without invasive blood collection, since
94first symptoms until seventh day of infection, even before appearing specific antibody [5].
95The major problem of using it is to find a NS1 protein specific to ZIKV without cross
96reaction with Dengue.

97Herein, we combine ZnO NRs-based working electrode with anti-ZIKV-NS1 protein
98antibody to detect ZIKV-NS1 antigen in urine without cross-reaction with Dengue. The
99developed diagnostic test is specific, cost-effective, takes short time and may be used as
100point-of-care device. The test is made in urine without filtration, and the biosensor can be
101read in a portable potentiostat. These characteristics make it ideal for using in borders of
102ports and airports for travelers who return from endemic areas. The test could also be part

103of prenatal care and used in health centers to identify patients with ZIKV. Furthermore, the
104obtained information by ZIKV biosensor could be used for management of the disease and
105identification of endemic areas.

106

1072. EXPERIMENTAL

108

1092.1. Materials and reagents

110The bare-sensor board was made by using a Printed Circuit Board Technology (PCB). The
111three electrode system was built on an FR-4 (1.6 mm thick) sheet (Jiangsu Sunyuan
112Aerospace Material Co).

113

1142.1.1. Chemical reagents and materials

115

116Zinc acetate, Hexamethylenetetramine (HMTA), zinc nitrate ($Zn(NO_3)_2$), buffered phosphate saline
117(PBS) pH7.4, Ferrocianeto de Potássio ($K_4[Fe(CN)_6]$) Nitrato de Sódio ($NaNO_3$), glycerol,
118bromophenol blue, and dithiothreitol solution were purchased from Sigma (St. Louis, MO). Silver
119Conductive Epoxy, H2OE EPO-TEK, were purchase from Epoxy Tecnology. Graphene oxide (GO)
120was prepared by modified Hummers' method [26]. Cystamine dihydrochloride (Cys, Alfa Aesar),
121Glutaraldehyde (Glut) 2.5% (Electron Microscopy Sciences) Prestained protein marker (Color-
122coded, Cell Signalling Tecnology). Nitrocellulose membrane (Bio-Rad, Hercules, CA). Transfer
123buffer consisting of 50 mM Tris-HCl, pH 7.0, 380 mM glycine, 0.1% SDS, and 20% methanol.
124Tris-buffered saline with Tween and incubated with horseradish peroxidase (HRP)-conjugated
125secondary antibody (Santa Cruz). Super Signal CL-HRP Substrate System (Pierce, Rockford, IL).

126

1272.1.2. Biological reagents

128Zika virus NS1 protein (Fitzgerald), mouse monoclonal anti-ZIKV-NS1 antibody (Fitzgerald);
129horseradish peroxidase (HRP)-conjugated secondary antibody (Santa Cruz); Dengue NS1 protein
130(DENV-NS1, Abcam – Cambridge).

131

1322.2. Electrochemical bare-sensor board fabrication

133

134Gold trails were used as working and counter electrodes, and silver trail as a reference
135electrode. Gold electrodes were deposited by an electrolytic method by using a current of
13620 A. The silver electrode was deposited by screen printed by using a Silver Conductive

137Epoxy, H2OE EPO-TEK and it was cured at 100°C for 2h. Figure S1 shows our
138electrochemical bare board made on FR-4 substrate.

139

1402.3. Growth of ZnO NRs on working electrode

141

142The samples were synthesized by CBD as previously described [26]. Firstly, a seeding
143layer, consisting of GO and zinc acetate films, was sprayed on the working electrode of the
144bare-sensor board by spray coating (Exacta Coat). Aiming to prepare it, we sprayed 12
145layers of a 0.05g.L⁻¹ GO solution followed by 12 layers of an ethanolic solution of 30
146mmol.L⁻¹ of zinc acetate. The spray parameters used during deposition were 5W, 1.00 KPa
147and 0.30 mL.min⁻¹ at 100 °C.

148After deposition of the seeding layer, samples were used for growing ZnO NRs by CBD.
149HMTA, and Zn(NO₃)₂ were mixed in the proportion 1:1 in a Polytetrafluoroethylene
150(PTFE) vessel. After that, the bare-sensor board was immersed in the precursor solution.
151The PTFE vessel was placed in silicone bath and the solution was stirred and heated at
15290°C for 2 h, aiming to promote the growth of ZnO NRs.

153

1542.4. Immobilization of the Zika NS1 antibody

155

156The monoclonal ZIKV-NS1 antibody (Ab) was immobilized via Cys 20mM and Glut 2.5%
157on the surface of ZnO NRs. Twenty microliters of anti-ZIKV-NS1 monoclonal antibody
158solution were diluted in 0.1M PBS pH7.4. Three different concentrations of dilution
159(1:10000, 1:5000 and 1:1000) were tested. The diluted solution was dropped on the surface
160of the working electrode and incubated for 12 hours at 4°C in a moist chamber.

161

1622.5. Electrochemical assays

163

164The analytical responses of the immunosensor were evaluated by electrochemical
165measurements by using cyclic voltammetry (CV). During CV assays, the potential was
166scanned from -0.7 to 0.7 V at the scan rate of 100 mV.s⁻¹ recorded in 10 mmol.L⁻¹
167K₄[Fe(CN)₆] and 0.5 mol.L⁻¹ NaNO₃ solution as mediator. All experiments were conducted
168in triplicate at room temperature.

169

1702.6. Characterization methods

171

1722.6.1 Structural and microstructural characterization

173All samples were characterized by Scanning Electron Microscopy (SEM) in a FEI Inspect
174F50 SEM microscope. Immunofluorescence Confocal Microscopy and Fourier Transform
175Infrared Spectroscopy (FTIR) were used to identify antibody binding to the surface sensor
176after immobilization. For the Immunofluorescence Confocal Microscopy analyzes, the
177sensors were incubated with Alexa Fluor 594 (Life Technologies) fluorescent secondary
178antibody for 1h at room temperature. The sensors were evaluated by fluorescence intensity
179in a confocal microscope Leica, model TCS SP5 II. The experiments were performed in a
180moist chamber. FTIR measurements were performed using an Attenuated Total
181Reflectance (ATR) accessory of the Thermo Scientific Smart iTR Nicolet iS10.

182

1832.6.2 Dot and Western blotting assays

184

185ZIKV-NS1 protein commercially available was characterized by western blotting. For this
186test, 200ng of recombinant Zika virus NS1 protein was spiked in 20 μ L of PBS. The
187samples were previously boiled at 95°C, with a 5% glycerol/ 0.03% bromophenol blue/10
188mM dithiothreitol solution, and loaded onto 10% SDS polyacrylamide gels. 10 μ L of
189prestained protein marker were used as standard. After electrophoresis, proteins were
190transferred to nitrocellulose membrane in a transfer buffer. The membranes were then
191incubated overnight at 4°C with primary antibodies, 1:5.000 mouse monoclonal anti-
192ZIKV-NS1 antibody. The blots were subsequently washed in Tris-buffered saline with
193Tween and incubated with HRP-conjugated secondary antibody. Immunoreactive bands
194were visualized with the enhanced chemiluminescence method (Super Signal CL-HRP
195Substrate System).

196

1972.7. Immunosensor performance for ZIKV-NS1 detection

198

199Immunosensor performance was evaluated by calibration curve and limit of detection
200(LoD). The ZIKV-NS1 standard was incubated in the immunosensor, and all analyses were
201performed according to followed protocol: after immobilization of the anti-ZIKV-NS1
202antibody, the immunosensor was incubated with different concentrations of ZIKV-NS1
203antigen (from 0.01-200 ng.mL⁻¹) at room temperature. Washing with PBS buffer was

204realized after each step to remove antibody or antigen excess. The incubation steps were
205performed in a moist chamber. The evaluation was performed by CV analysis.

206

2072.8. Immunosensor Specificity for ZIKV-NS1

208

209The specificity of the ZIKV-NS1 immunosensor was assessed regarding Dengue NS1
210protein (DENV-NS1) sample. $2.0\mu\text{g}\cdot\text{mL}^{-1}$ DENV-NS1 was diluted in PBS buffer, dropped
211upon sensors, and incubated during 60 min. Afterward, the sensors were characterized by
212CV analysis.

213Recombinant Zika virus NS1 protein and Recombinant Dengue virus 1 NS1 protein were
214characterized for dot blot analysis. A nitrocellulose membrane, and draw a grid by pencil
215were used to indicate the region we went blot. Using pipette tip, we spotted $2\mu\text{l}$ of samples
216onto the nitrocellulose membrane at the center of the grid. The dots were made with $1.5\mu\text{g}$;
217 $0.15\mu\text{g}$; $0.015\mu\text{g}$, 1.5ng and 0.15ng . The membranes were let to dry for 30 min, and
218incubated overnight at 4°C with 1:5.000 mouse monoclonal anti-ZIKV-NS1 antibody. The
219blots were subsequently washed in Tris-buffered saline solution with Tween and incubated
220with HRP-conjugated secondary antibody. Immunoreactive bands were visualized with the
221enhanced chemiluminescence method.

222

2232.9. Urine samples analyses

224

225The urine samples used here were supplied by the author herself. All methods were carried
226out in accordance with guidelines and regulations of the National Committee on Research
227Ethics, CONEP/CNS/MS, of the Brazil. All experimental protocols were approved by
228Comissão Nacional de Ética em Pesquisa – CONEP/CNS/MS. The human urine samples
229were collected in sterile means and immediately used. Before CV analysis, the undiluted
230urine sample was spiked with ZIKV-NS1 protein in urine with 02 different concentrations
231($0.01\mu\text{g}\cdot\text{mL}^{-1}$ and $2.0\mu\text{g}\cdot\text{mL}^{-1}$). The sensors were incubated in the urine samples during 60
232min and characterized by CV analysis. For western blotting, 200ng of recombinant Zika
233virus NS1 protein was spiked in $20\mu\text{L}$ of PBS, diluted urine in PBS (1:10) or undiluted
234urine. The western blotting was performed as described above.

235

2363. RESULTS

237

2383.1 Characterization of the bare board sensor

239

240 ZnO NRs are excellent semiconductors used for anchoring biomolecules, as antibodies, in
241 its surface [21]. On the other hand, (Au) gold is another excellent material used for
242 immobilize antibodies in biosensors. As our bare board sensor has working-electrode and
243 trails made with Au film, we performed some immobilization tests in it, before growing
244 ZnO NRs. The idea was to identify if the gold could contribute in the immobilization of
245 antibodies. Figure 1a-b shows CV curves obtained for pure and incubated with Cys, Glut
246 and anti-NS-1 antibody of ZIKV bare boards, respectively. No differences are observed in
247 the curves and anodic peaks (I_{pa}) values in the presence of the ZIKV NS1 for both boards.
248 That means there was no immobilization of the antibody in the bare board sensor before
249 growing ZnO NRs. The lower surface area of the gold film may be contributed for it.
250 The stability of our homemade bare board sensor was evaluated by successive cyclic
251 voltammograms performed in the presence of 10mmol.L^{-1} of $\text{K}_4[\text{Fe}(\text{CN})_6]$ prepared in 0.5
252 mol.L^{-1} NaNO_3 electrolyte at 100mV.s^{-1} scanning rate and potential ranging from -0.7 to
253 7.0V (Figure 1c). The redox peaks were basically constant even after 10 cycles. Coefficient
254 of variation, calculated based in I_{pa} , was 2.5%, validating the excellent stability of our
255 homemade bare board sensor.

256

2573.2 Growth of ZnO NRs on working electrode

258

259 After growing of ZnO NRs upon working electrode of the bare board, the samples were
260 characterized by SEM (Figure 1d and e). Micrographs show ZnO NRs grow
261 perpendicularly to the board with good density, as previously reported [21]. Because of the
262 higher surface, using ZnO NRs can be a good path to immobilize antibodies and increase
263 the selectivity and limit of detection of the biosensor.

264

265 Please insert Figure 1 here

266

2673.3 Anti-ZIKV-NS1 immobilization

268

269 The sensor specificity is strongly related to the properties of the immobilized detection
270 element [14]. The use of antibodies is an excellent tool for making biosensors because they
271 are highly specific [22].

272 Before anti-ZIKV-NS1 immobilization on the board sensor, it is necessary to evaluate the
273 specificity of antibody-antigen linkage used here. For this, we performed a Western
274 blotting analysis using a 200ng of isolate ZIKV-NS1 protein (Figure 2a). Only one band,
275 around 50 kDa, appears in the analysis. The result indicates the purity of the ZIKV-NS1
276 protein and the high selectivity of antibody.

277 After testing the specificity of ZIKV-NS1 protein, we immobilized it via Cys and Glut
278 2.5% on the surface of ZnO NRs grown on the board sensor. Firstly, Cys (an organic
279 amine disulfide) binds to oxygen dominant species on ZnO NRs surface via thiol groups,
280 and modified it with amino groups. Subsequently, Glut covalently binds to amino groups
281 and providing carbonyl groups on the sensor surface. Afterward, the amino groups (NH₂-
282 Y) of the antibodies easily bind to the carbonyl groups.

283 One of the crucial parameters on developing low-cost biosensors is using small quantities
284 of antibodies as possible. Therefore, we tested the immobilization of antibody with three
285 different concentrations (1:1000; 1:5000 and 1:10000). The CV curves reveal a reduction
286 in the I_{pa} values with addition of cys, glut or antibodies due to isolating nature of these
287 compounds (Figure 2b). Incubating the sensor with lower antibody concentration (1: 5000
288 or 1: 10000) still resulted in a decrease of the I_{pa} compared to that immobilized just with
289 cys and glu (Fig 2b). That means the immobilization of the antibody at the bare board
290 sensor also occur in these concentrations. As the use of lower antibody concentration may
291 reduce the cost of production, we choose the 1: 5000 for sensor assembly.

292

293 3.3.1 Characterization of Anti-ZIKV-NS1 immobilization on the board sensor

294

295 Antibody immobilization upon bare board sensor was confirmed by Confocal Fluorescence
296 Microscopy. An intense fluorescence was observed in the board sensor with Ab
297 immobilization (Figure 2e) when compared to sensor without Ab immobilization (Figure
298 c and d).

299 Regarding the FTIR data, Figure 2f, the antibody immobilization was confirmed by the
300 appearance of well define bands around 2093 cm⁻¹ and 1352 cm⁻¹ that could be attributed
301 to the stretching vibration of the C≡N bond and N=O respectively [27]. The NS-1 ZIKV
302 protein immobilization was confirmed by increase in peaks of band around 2093 cm⁻¹ and
303 1352 cm⁻¹, suggesting a correct antibody orientation.

304 We evaluated the stability of immunosensor and observed a good repeatability of I_{pa}
305 (6.5% coefficient of variation) in ten sequential voltammograms curves (Figure S2).

306 Another advantage of our immunosensor as a rapid test is reproducibility. We assessed this
307 parameter in four ZIKV-NS1 immunosensors and observed I_{pa} values very similar (4.5%
308 coefficient of variation) (Figure 2g).

309

310 Please insert Figure 2 here

311

312 3.4 Characterization of the ZIKV-NS1 Immunosensor

313

314 Under optimized experimental conditions, the calibration curve of immunosensor was
315 performed with electrodes incubated in different concentrations of ZIKV-NS1 and
316 submitted to CV analyses in presence of $K_3[Fe(CN)_6]/K_4[Fe(CN)_6]$ (10mM) in $NaNO_3$
317 (0.5 mol.L^{-1}). The results show that the I_{pa} increase by increasing of ZIKV-NS1
318 concentration in incubation solution (Figure 3a). Probably, a reaction between antibody
319 with ZIKV-NS1 occurs with charge transfer. Good linearity in the calibration curve was
320 obtained over the range 0.1 ng.mL^{-1} to 100 ng.mL^{-1} of ZIKV-NS1 ($r^2 = 0.9536$; $n = 4$)
321 (Figure 3b). This linearity is suitable with ZIKV tests previously authorized by Food and
322 Drug Administration (FDA) [28]. The purpose of our device is providing a rapid test to
323 detect ZIKV-NS1 protein. As ZIKV-NS1 is an exogenous protein, not produced
324 physiologically by the human body, using a fast qualitative test should be appropriated for
325 detecting Zika without cross-reaction with Dengue.

326 The Limit of Detection is lower than 1 pg.mL^{-1} (Figure 3c), indicating our ZnO NRs-based
327 immunosensor is a good rapid test for detection of ZIKV in beginning of disease.

328 Some differences of potential can be seen in CV analyses. Probably, these differences are
329 related with more random or oriented Ab immobilized on the surface of ZnO NRs. We
330 worked with batches of samples and the surface pKa, temperature and humidity of the day
331 may affect the orientation of the Ab onto ZnO NRs surface in these batches, since the
332 immobilization occurs by adsorption. In addition, there are a number of intermediate states
333 of immobilization that may either lead to reduced access of the cognate antigen to the Ab-
334 binding site or link the Ab close to this site with an associated reduction in binding.

335 Despite these limitations, within the same batch, the samples show the identical behavior;
336 that is, the I_{pa} increase by increasing of ZIKV-NS1 concentration. For each batch, we
337 analyzed a control sample.

338

339 Please insert Figure 3 here

340

341 In order to determine the optimum incubation period of the ZIKV-NS1 antigen (Ag), we
342 tested times of 10, 30 and 60 min for incubating $0.01 \mu\text{g.mL}^{-1}$ ZIKV-NS-1. A higher anodic
343 peak is observed for incubation periods higher than 30 min (Figure 4a). Incubation period
344 higher than 30min favor a better charge transfer process during linkage of the antigen
345 (Figure 4b).

346

347 Please insert Figure 4 here

348

349 3.5 ZIKV-NS1 Immunosensor Cross Reaction

350

351 The cross-reaction between DENV-NS1 and ZIKV-NS1 is very common since the protein
352 sequence identities in the 53-56% range [29]. Because this DENV-NS1 was chosen to
353 evaluate the specificity of immunosensor. The specificity of our ZIKV-NS1
354 immunosensor regarding dengue as assayed, and recovery experiments were carried out by
355 adding $2.0 \mu\text{g.mL}^{-1}$ DENV-NS1 (Figure 5a). CV curves showed similar Ipa values even in
356 the presence of high level of DENV-NS1 antigen. That means DENV-NS1 antigen didn't
357 link with anti-ZIKV-NS1 antibody and confirm the specificity of our immunosensor. Dot-
358 blot assay using ZIKV-NS1 and DENV-NS1 antigen incubated with anti-ZIKV-NS1
359 antibody (1:5000) (Figure 5b) also endorsed non-reactivity of our immunosensor with
360 Dengue antigen.

361

362 Please insert Figure 5 here

363

364 3.6 Analysis of spiked human urine samples

365

366 Previous groups have reported tests in urine to detect flavivirus, such as DENV [30], West
367 Nile virus [31] and ZIKV [32, 33]. Using urine for disease diagnoses has some advantages,
368 such as noninvasive sampling and ease of use. To confirm if the antibody-antigen binding
369 remains in the urine samples, we performed the Western blotting assay (Figure 6a). Four
370 samples were prepared: PBS spiked with 200ng ZIKV-NS1, Urine diluted in PBS (1:10)
371 spiked with 200ng ZIKV-NS1, undiluted urine spiked with 200ng ZIKV-NS1 and urine.
372 We observed a single band at 50KDa, revealing no interference by the other compounds of

373the urine in antigen-antibody linking. Urine samples were assessed, and CV recovery
374experiments were carried out via the standard addition method. Assuming a null
375concentration of ZIKV-NS1 in the urine sample, CVs curves showed the possibility for
376detecting ZIKV-NS1 in urine without interference of its compounds (Figure 6b). To
377corroborate with this findings we analyze undiluted urine and undiluted urine spiked with
378 $0.01\mu\text{g}/\text{mL}^{-1}$ and $2.0\mu\text{g}/\text{mL}^{-1}$ of ZIKV-NS1 and observed the immunosensor is capable
379to detect ZIKV-NS1 in urine even in the presence of interference compounds (Figure S3).
380

381Please insert Figure 6 here

382

383The diagnosis of ZIKV has been routinely carried out through the genome viral detection
384or by serological tests identifying IgG and IgM antibodies [4]. The disadvantages of these
385validation techniques in relation to our device is on the detection of IgG and IgM, which is
386done later (from the fourth to the 6th day after the onset of symptoms) [34]. In addition, the
387similarity of the DENV and ZIKV viruses allows the frequent occurrence of cross-reaction,
388evidencing the low specificity of the tests [34]. The techniques that evaluate the viral
389genome are accurate, RT-PCR is considering the gold standard for ZIKV detection, but
390like serology, they are carried out in clinical analysis laboratories. Therefore, they are
391expensive and time consuming. Our ZnO NRs-based electrochemical immunosensor can
392be used as a POC disposable, is able for detection ZIKV from the first day of symptoms, in
393a specific way (without cross-reaction with DENV), is selective, and the result can be
394obtained within one hour after collect of material. The sample used is undiluted urine with
395no processing required. The immunosensor can be read in a portable potentiostat and could
396be part of prenatal care and used in health centers to identify patients with ZIKV.

397

3984. CONCLUSION

399

400A ZnO NRs-based electrochemical immunosensor was successfully applied here as a rapid
401test for detection of ZIKV infection in urine. The biosensor showed high specificity to
402ZIKV-NS1, without cross-reactive with Dengue, and low limit of detection ($1.00\text{ pg}\cdot\text{mL}^{-1}$).
403Dot-blot assay endorsed non-reactivity of our ZnO NRs-based immunosensor with Dengue
404antigen. Taking the test in urine enables the immunosensor to be performed as a rapid
405point-of-care test without need experts. The immunosensor here showed stability and

406reproducibility suitable with other ZIKV tests. In the next steps, we are going to validate
407our immunosensor by analyzing patient urine samples. The obtained results will be
408compared to them gold standard test (RT-PCR). The immunosensor here developed has
409significant potential to improve early diagnostics of ZIKV, including weak healthcare
410infrastructure areas.

411

412

4135. Author Contributions

414**Aline M. Faria:** Methodology, Validation, Formal Analyses, Writing-Original Draft
415preparation. **Talita Mazon:** Conceptualization, Writing-Reviewing and Editing,
416Supervision.

417

418

4196. Acknowledgements

420The authors would like to be thankful to CNPq and the Center for Research Brazilian
421Agencies and the CMF/CEPID/ FAPESP by the financial support. The LME/LNNano –
422Brazilian Nanotechnology National Laboratory/CNPEM/MCTI by the support in SEM
423images. We thank the staff of the Electronic Packaging from CTI for the support on
424fabrication our homemade bare-sensor board. We also thank the staff of the Life Sciences
425Core Facility (LaCTAD) from State University of Campinas (UNICAMP), for the
426Confocal Microscopy analysis. In particular, the authors are grateful to Dr. José Butori
427Lopes de Faria (Renal Pathophysiology Laboratory, Investigation on Diabetes
428Complications, Faculty of Medical Sciences, State University of Campinas - UNICAMP)
429for his technical and scientific assistance.

430

431

432**7. Competing Interests:** The authors declare that they have no competing interests.

433

434**8. Additional Information:** Supplementary information accompanies this paper.

435

4369. References

437

438[1] M.R. Duffy, T.H. Chen, W.T. Hancock, A.M. Powers, J.L. Kool, R.S. Lanciotti,
439M.Pretrick, M. Marfel, S. Holzbauer, C. Dubray, L. Guillaumot, A. Griggs, M. Bel, A.J.

- 440 Lambert, J. Laven, O. Kosoy, A. Panella, B. J. Biggerstaff, M. Fischer, E.B. Hayes. Zika
441 virus outbreak on Yap Island, Federated States of Micronesia. *N. Engl. J. Med.* 360 (2009)
442 2536–2543. <http://dx.doi.org/10.1056/NEJMoa0805715>.
- 443 [2] J. J. Waggoner, L. Gresh, A. Mohamed-Hadley, G. G. Ballesteros, M. J. V. Davila, Y.
444 Tellez, M.K.Sahoo, A. Balmaseda, E. Harris, B. A. Pinsky. Single-Reaction Multiplex
445 Reverse Transcription PCR for Detection of Zika, Chikungunya, and Dengue Viruses.
446 *Emerging Infectious Diseases*. 22 (2016) 1295-1297.
- 447 [3] D. Musso, D.J. Gubler. Zika Virus. *Clin. Microbiol. Rev.* 29 (2016). 487-503.
- 448 [4] T.B. Casale, M.N. Teng, J.P. Morano, T. Unnasch, J. Charles, C.J. Lockwood. Zika
449 virus: An emerging infectious disease with serious perinatal and neurologic complications.
450 *J. Allergy Clin. Immunol.* 141 (2018) 482-490. <https://doi.org/10.1016/j.jaci.2017.11.029>
- 451 [5] CDC. Guidance for U.S. Laboratories Testing for ZIKV Infection. Available at:
452 <https://www.cdc.gov/zika/laboratories/lab-guidance.html>. Accessed June 21, 2018.
- 453 [6] World Health Organization. Zika virus disease - diagnosis. Available at:
454 <http://www.who.int/csr/disease/zika/en>. Accessed June 21, 2018.
- 455 [7] K. Steinhagen, C. Probst, C. Radzimski, J. Schmidt-Chanasit, P. Emmerich, M. van
456 Esbroek, J. Schinkel, M.P. Grobush, A. Goorhuis, J.M. Warnecke, E. Lattwein, L.
457 Komorowski, A. Deerbeg, S. Saschenbrecker, W. Stocker, W. Schlumberger.
458 Serodiagnosis of Zika virus (ZIKV) infections by a novel NS1-based ELISA devoid of
459 cross-reactivity with dengue virus antibodies: a multicohort study of assay performance,
460 2015 to 2016. *Euro Surveill.* 15 (2016) 1-16. doi: 10.2807/1560-7917.ES.2016.21.50.30426.
- 461 [8] C. Myhrvold, C. A. Freije, J.S. Gootenberg, O.O. Abudayyeh, H.C. Metsky, A.F.
462 Durbin, M.J. Kellner, A.L. Tan, L.M. Paul, L.M., L.A. Parham, K.F. Garcia, K.G. Barnes,
463 B. Chak, A. Mondini, M.L. Nogueira, S. Isern, S.F. Michael, I. Lorenzana, N.L. Yozwiak,
464 B.L. MacInnis, I. Bosch, L. Gehrke, F. Zhang, P.C. Sabeti. Field-deployable viral
465 diagnostics using CRISPR-Cas13. *Science* 360 (2018). 444-448. doi:
466 [10.1126/science.aas8836](https://doi.org/10.1126/science.aas8836).
- 467 [9] J. Song, M.G. Mauk, B.A. Hackett, S. Cherry, H.H. Bau, C. Liu. Instrument-Free
468 Point-of-Care Molecular Detection of Zika Virus. *Anal. Chem.* 88 (2016) 7289-7294. doi:
469 [10.1021/acs.analchem.6b01632](https://doi.org/10.1021/acs.analchem.6b01632).
- 470 [10] I. Bosch, H. de Puig, M. Hiley, M. Carré-Camps, F. Perdomo-Celis, C.F. Narváez, C.
471 F., et al. Rapid antigen tests for dengue virus serotypes and Zika virus in patient serum.
472 *Sci. Transl. Med.* 9 (2017) eaan1589. doi: 10.1126/scitranslmed.aan1589.

- 473[11] C. Shan, X. Xie, P. Ren, M. J. Loeffelholz, Y. Yang, A. Furuya, , A.P. Dupuis, L.D.
474Kramer, S.J. Wong, J. Susan, P.Y. Shi. A rapid Zika diagnostic assay to measure
475neutralizing antibodies in patients. *EBioMedicine* 17 (2017) 157–162. doi:
47610.1016/j.ebiom.2017.03.006.
- 477[12] H. Song, J. Qi, J. Haywood, Y. Shi, G.F. Gao, Zika virus NS1 structure reveals
478diversity of electrostatic surfaces among flaviviruses. *Nat. Struct. Mol. Biol.* 23 (2016b).
479456-458.
- 480[13] A. Sassolas, L.J., Blum, B.D. Leca-Bouvier, Immobilization strategies to develop
481enzymatic biosensors. *Biotechnol. Adv.* 30 (2012) 489–571.
- 482[14] E.L. Lewandrowski, K. Lewandrowski. Implementing point-of-care testing to improve
483outcomes. *J. Hosp. Adm.* 2 (2013) 125-132.
- 484[15] M. Bhattacharya, S. Hong, D. Lee, T. Cui, S.M. Goyal. Carbon nanotube based
485sensors for the detection of viruses. *Sensors and Actuators B: Chemical.* 155 (2011) 67-74.
486<https://doi.org/10.1016/j.snb.2010.11.025>
- 487[16] S. Afsahi, M.B. Lerner, J.M. Goldstein, J. Lee, X. Tang, D.A. Bagarozzi Jr., D. Pan, L.
488Locascio, A. Walkera, F. Barron, R. Brett, B.R. Goldsmith. Novel graphene-based
489biosensor for early detection of Zika virus infection. *Biosensors and Bioelectronics* 100
490(2018) 85–88. <http://dx.doi.org/10.1016/j.bios.2017.08.051>
- 491[17] M.M.S. Silva, A.C.M.S. Dias, M.T. Cordeiro, E. Marques Jr, M.O.F. Goulart , R.F.
492Dutra. A thiophene-modified screen printed electrode for detection of dengue virus
493NS1protein. *Talanta* 128 (2014) 505–510. <http://dx.doi.org/10.1016/j.talanta.2014.06.009>
- 494[19] Y. Anno, T. Maekawa, J. Tamaki, Y. Asano, K. Hayashi, N. Yamazoe. Zinc-oxide-
495based semiconductor sensors for detecting acetone and capronaldehyde in the vapour of
496consomme´ soup. *Sensors and Actuators B: Chemical.* 25 (1995) 623-627.
497[https://doi.org/10.1016/0925-4005\(95\)85137-2](https://doi.org/10.1016/0925-4005(95)85137-2)
- 498 [20] Q. Rui, K. Komori, Y. Tian, H. Liu, Y. Luo, Y. Sakai. Electrochemical biosensor for
499the detection of H₂O₂ from living cancer cells based on ZnO nanosheets. *Anal. Chimica*
500Acta. 670 (2010). 57-62.
- 501[21] G. Gasparotto, J.P.C. Costa, P.I. Costa, M.A. Zaghete, T. Mazon. Electrochemical
502immunosensor based on ZnO nanorods-Au nanoparticles nanohybrids for ovarian cancer
503antigen CA-125 detection. *Mat. Sci and Engin. C.76* (2017). 1240–1247.
504<https://doi.org/10.1016/j.msec.2017.02.031>
- 505[22] S. Sharma, H. Byrne, R.J. O’Kennedy. Antibodies and antibody-derived analytical
506biosensors. *Essays in Biochem.* 60 (2016) 9–18.

- 507[23] X. Xu, H. Song, J. Qi, Y. Yuqian Liu, H. Wang, C. Su, Y. Shi, G. Gao. Contribution
508of intertwined loop to membrane association revealed by Zika virus full-length NS1
509structure. *The EMBO J.* 35 (2016) 2170 – 2178. DOI 10.15252/embj.201695290.
- 510[24] D.A. Muller, P.R. Young. The flavivirus NS1 protein: molecular and structural
511biology, immunology, role in pathogenesis and application as a diagnostic biomarker.
512*Antiviral Res.* 98 (2013) 192-208. DOI: 10.1016/j.antiviral.2013.03.008 PMID: 23523765.
- 513[25] W.C. Brown, D.L. Akey, J.R. Konwerski, J.T. Tarrasch, G. Skiniotis, R.J. Kuhn,
514J.L. Smith. Extended surface for membrane association in Zika virus NS1 structure. *Nat.*
515*Struct. Mol. Biol.* 23 (2016) 865-867. DOI: 10.1038/nsmb.3268 PMID: 27455458
- 516 [26] B.A. Vessalli, C.A. Zito, T.M. Perfecto, D. P. Volanti, T. Mazon. ZnO
517nanorods/graphene oxide sheets prepared by chemical bath deposition for volatile organic
518compounds detection. *J. of Alloys and Compounds*, 696 (2017) 996–1003.
519<https://doi.org/10.1016/j.jallcom.2016.12.075>
- 520[27] A.E. Segneanu, I. Gozescu, A. Dabici, P. Sfirloaga, Z. Szabadai. *Organic Compounds*
521*FT-IR Spectroscopy, Macro To Nano Spectroscopy*, Dr. Jamal Uddin (2012). ISBN: 978-
522953-51-0664-7, InTech, Available from: [http://www.intechopen.com/books/macro-to-](http://www.intechopen.com/books/macro-to-nanospectroscopy/organiccompounds-ft-ir-spectroscopy)
523*nanospectroscopy/organiccompounds-ft-ir-spectroscopy*.
- 524[28] U.S. Food and Drug Administration (FDA).
525[https://www.fda.gov/EmergencyPreparedness/Counterterrorism/MedicalCountermeasures/](https://www.fda.gov/EmergencyPreparedness/Counterterrorism/MedicalCountermeasures/MCMIssues/ucm485199.htm#products)
526[MCMIssues/ucm485199.htm#products](https://www.fda.gov/EmergencyPreparedness/Counterterrorism/MedicalCountermeasures/MCMIssues/ucm485199.htm#products). Accessed August 14, 2018.
- 527[29] H. Song, J. Qi, J. Haywood, Y. Shi, G.F. Gao. Zika virus NS1 structure reveals
528diversity of electrostatic surfaces among flaviviruses. *Nat. Struct. Mol. Biol.* 23 (2016)
529456–458.
- 530[30] T., Hirayama, Y. Mizuno, N. Takeshita, A. Kotaki, S. Tajima, T. Omatsu, K. Sano, I.
531Kurane, T. Takasaki. Detection of dengue virus genome in urine by real-time reverse
532transcriptase PCR: a laboratory diagnostic method useful after disappearance of the
533genome in serum. *J. Clin. Microbiol.* 50 (2012) 2047–2052.
534<http://dx.doi.org/10.1128/JCM.06557-11>
- 535[31] L. Barzon, M. Pacenti, E. Franchin, S. Pagni, T. Martello, M. Cattai, et al. Excretion
536of West Nile virus in urine during acute infection. *J. Infect. Dis.* 208 (2013) 1086–1092.
537<http://dx.doi.org/10.1093/infdis/jit290>

538[32] S. Kutsuna, Y. Kato, T. Takasaki, M. Moi, A. Kotaki, H. Uemura, et al. Two cases of
539Zika fever imported from French Polynesia to Japan, December 2013 to January 2014.

540Euro Surveill. 19 (2014) pii:20683.

541[33] A.-C. Gourinat, O. O'Connor, E. Calvez, C. Goarant, M. Dupont-Rouzeyrol. Detection
542of Zika Virus in Urine. *Emerging Infectious Diseases*, 21 (2015) 84–86.

543<http://doi.org/10.3201/eid2101.140894>

544[34] C. Eppes, M. Rac, J. Dunn, J. Versalovic, K.O. Murray, M.A. Suter, M.S. Cortes, J.
545Espinoza, M.D. Seferovic, W. Lee, P. Hotez, J. Mastrobattista, S.L. Clark, M.A. Belfort,
546K.M. Aagaard. Testing for Zika virus infection in pregnancy: key concepts to deal with an
547emerging epidemic. *American Journal of Obstetrics & Gynecology*. 216 (2017) 209-225.
548doi: 10.1016/j.ajog.2017.01.020.

549

550

551

552 FIGURE CAPTIONS

553

554 Figure 1: a) Cyclic voltammogram (CV) obtained for Bare board. b) CV obtained for Bare
555 board plus antibody. c) CV obtained for FR-4 bare-sensor board with 10 scans. All cyclic
556 voltammograms (CVs) were performed with a scan rate of $100\text{mV}\cdot\text{s}^{-1}$. d) SEM image of the
557 ZnO nanostructures grown on sensor board, magnitude 5000x. e) SEM image of the ZnO
558 nanostructures grown on sensor board, magnitude 50000x.

559

560 Figure 2: a) Western blotting analyzes for ZIKV-NS1 showing the ZIKV-NS1 protein
561 purity, 50KDa size, and the good selectivity of antibody. b) CVs obtained in different steps
562 of preparing the immunosensor. c-e) Fluorescence Confocal Micrograph. c) Bare sensor
563 board without GO/ZnO-NRs. d) Sensor board with GO/ZnO-NRs. e) sensor board with
564 GO/ZnO-NRs plus antibody immobilization. All sensors were incubated with fluorescent
565 secondary antibody. f) FTIR spectra in bare board (Black), in immunosensor (Blue) and in
566 immunosensor incubated with NS-1 ZIKV protein (Red). g) CVs obtained for different
567 immunosensors showing their reproducibility. All CVs were performed with a scan rate of
568 $100\text{mV}\cdot\text{s}^{-1}$.

569

570 Figure 3: a) Voltammograms obtained for immunosensors in different ZIKV-NS1
571 concentrations. b) Linearity of calibration curve obtained over the range $0.01\text{ ng}\cdot\text{mL}^{-1}$ to
572 $100\text{ ng}\cdot\text{mL}^{-1}$ of NS-1 Zika Virus protein ($r=0.9536$). c) CVs of immunosensor incubated
573 with different ZIKV-NS1 concentrations. All CVs were performed with a scan rate of
574 $100\text{mV}\cdot\text{s}^{-1}$.

575

576 Figure 4: a) CVs obtained for Zika-NS1 immunosensors incubated with antigen
577 (Ag) (Zika-NS1 protein standard - $0.01\mu\text{g}\cdot\text{mL}^{-1}$); in black without Ag incubation; in red
578 10 min of Ag incubation; 30 min of Ag incubation; green and blue 60 min of Ag
579 incubation. All CVs were performed with a scan rate of $100\text{mV}\cdot\text{s}^{-1}$. b) Graphical
580 representation of $I_{pa} \times \text{time}$.

581

582 Figure 5: a) Voltammograms obtained by CV analyzes of immunosensors in presence of
583 $2.0\mu\text{g}\cdot\text{mL}^{-1}$ of DENV-NS1 antigen at scanning rate of $100\text{mV}\cdot\text{s}^{-1}$. b) Dot blot for ZIKV-

584NS1 and DENV-NS1 antigen in different concentrations incubated with antibody anti-
585ZIKV-NS1(1:5000). All CVs were performed with a scan rate of $100\text{mV}\cdot\text{s}^{-1}$.

586

587Figure 6: a) Western blotting assay to access the ZIKV-NS1 expression: lane 1 - PBS
588spiked ZIKV-NS1(200ng); lane 2 - Urine Diluted in PBS (1:10) spiked ZIKV-NS1(200ng);
589lane 3 - Urine Diluted in PBS (1:10) spiked ZIKV-NS1(200ng); lane 4 - Urine. b)
590Voltammograms obtained by CV analyzes of immunosensors incubated with undiluted
591urine. In black CV of immunosensor incubated with urine without ZIKV-NS1; in red CV
592of immunosensor incubated with urine plus ZIKV-NS1 ($0.01\mu\text{g}\cdot\text{mL}^{-1}$); in green CV of
593immunosensor incubated with urine plus ZIKV-NS1 ($2.0\mu\text{g}\cdot\text{mL}^{-1}$). All CVs were
594performed with a scan rate of $100\text{mV}\cdot\text{s}^{-1}$.

595

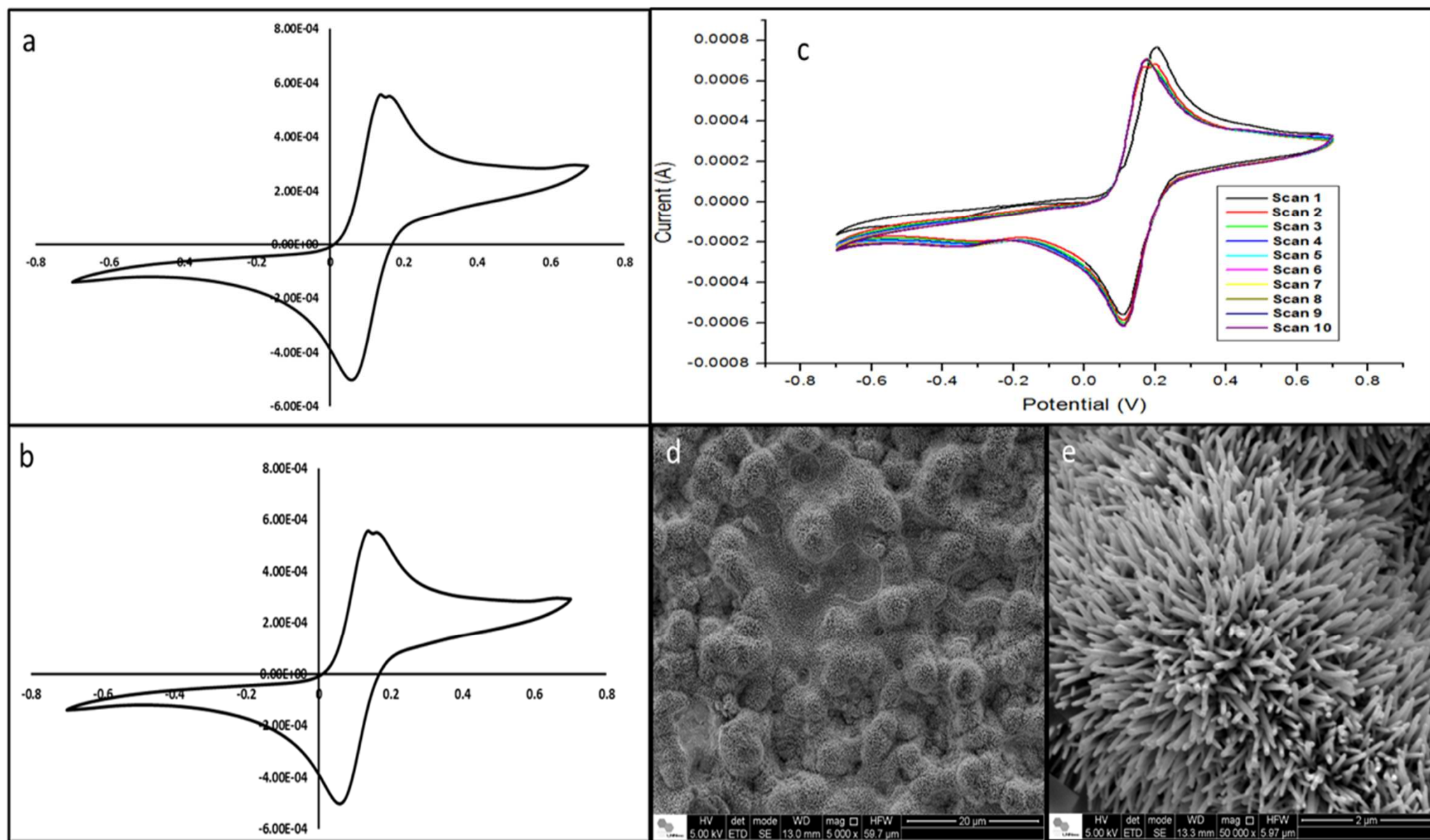
596Supplementary Material: Figure S1: The bare-sensor board was made on FR-4 (1.6 mm
597thick) sheets using a Printed Circuit Board Technology (PCB). It was composed of gold
598trails (Au) as working and counter electrode, and silver (Ag) as a reference electrode, being
599configured each to be electrically isolated from the others. The working electrode is
600composed of ZnO nanostructures on the Au trail. Figure S2: Cyclic voltammogram of our
601immunosensor with 10 scans performed with a scan rate of $100\text{mV}\cdot\text{s}^{-1}$. Figure S3: Cyclic
602voltammogram of ZIKV-NS1 immunosensor incubated with urine (black) and urine + 0.01
603 $\mu\text{g}\cdot\text{mL}^{-1}$ ZIKV-1 (red) . Scan rate of $100\text{mV}\cdot\text{s}^{-1}$.

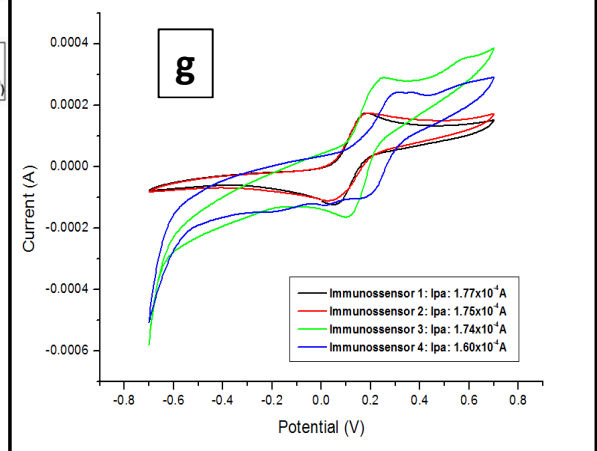
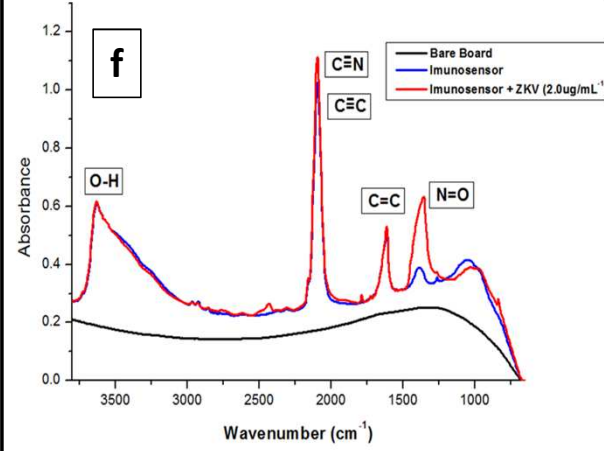
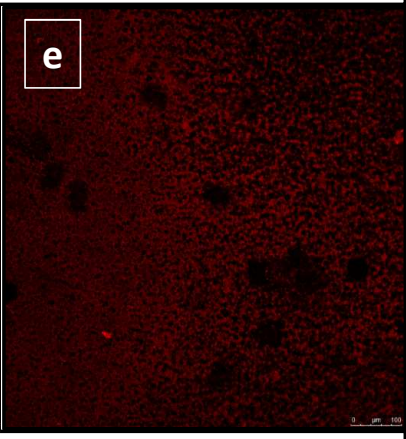
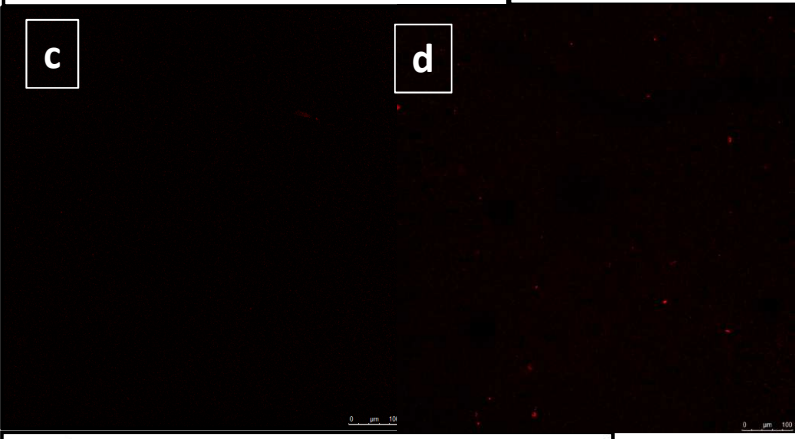
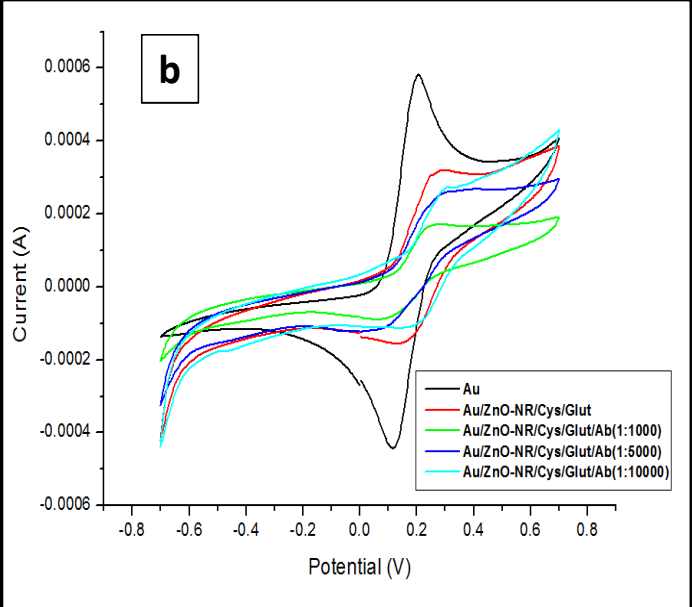
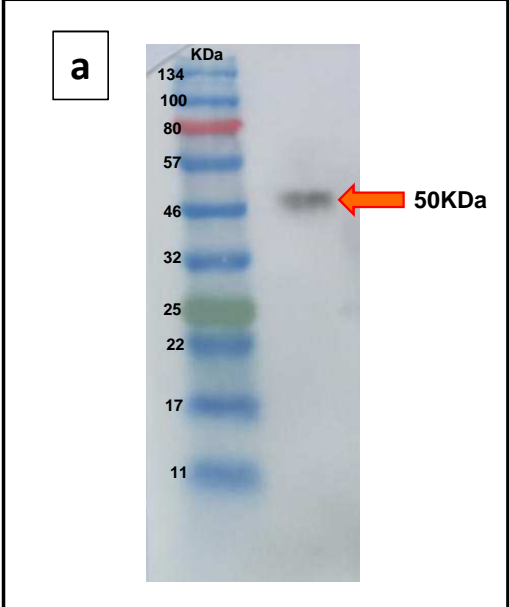
604

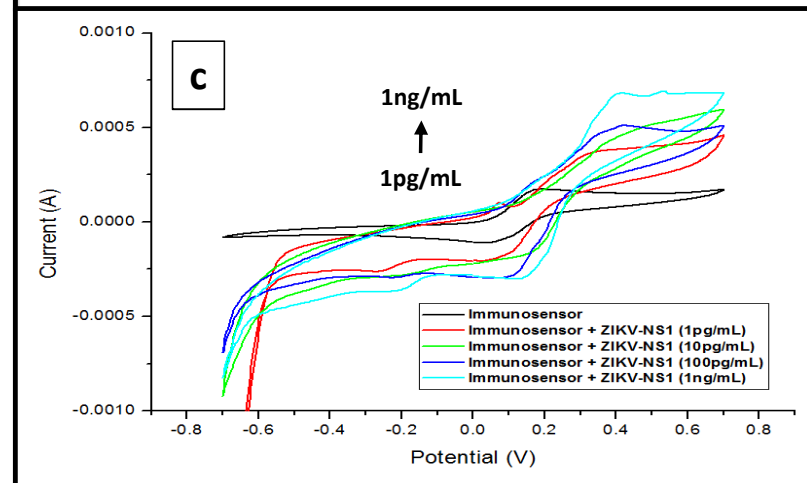
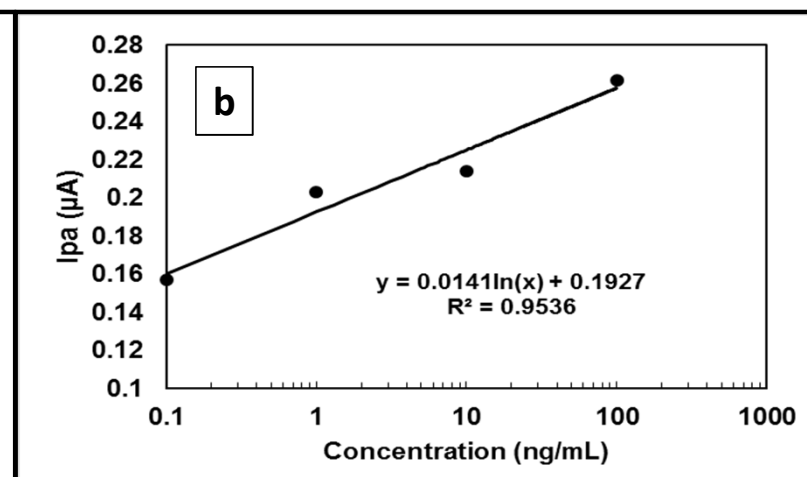
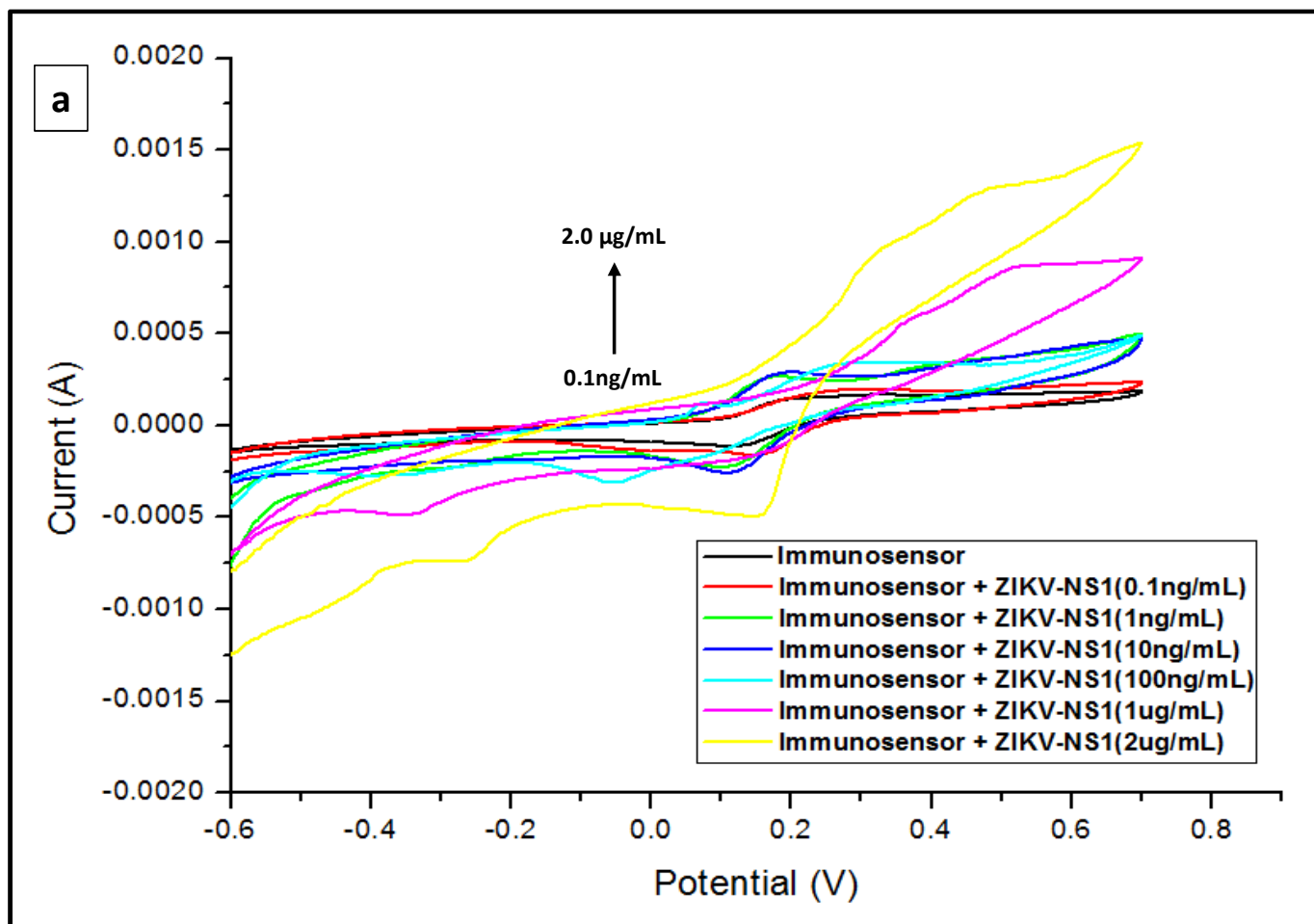
605

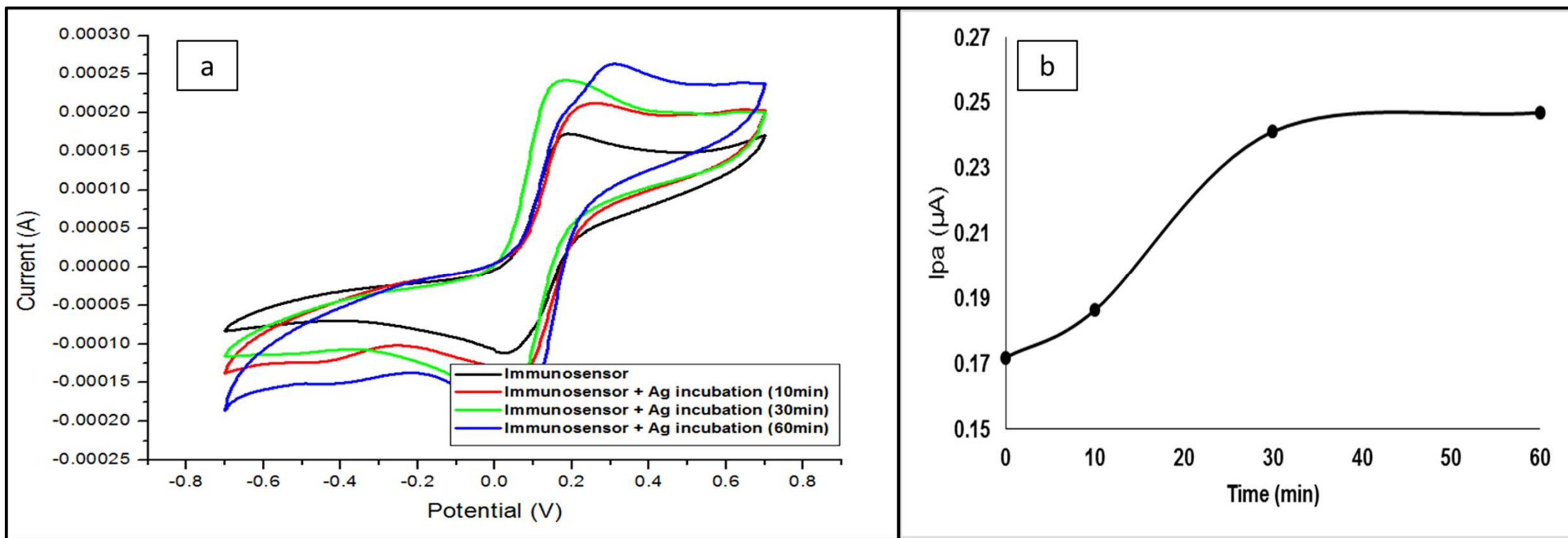
606

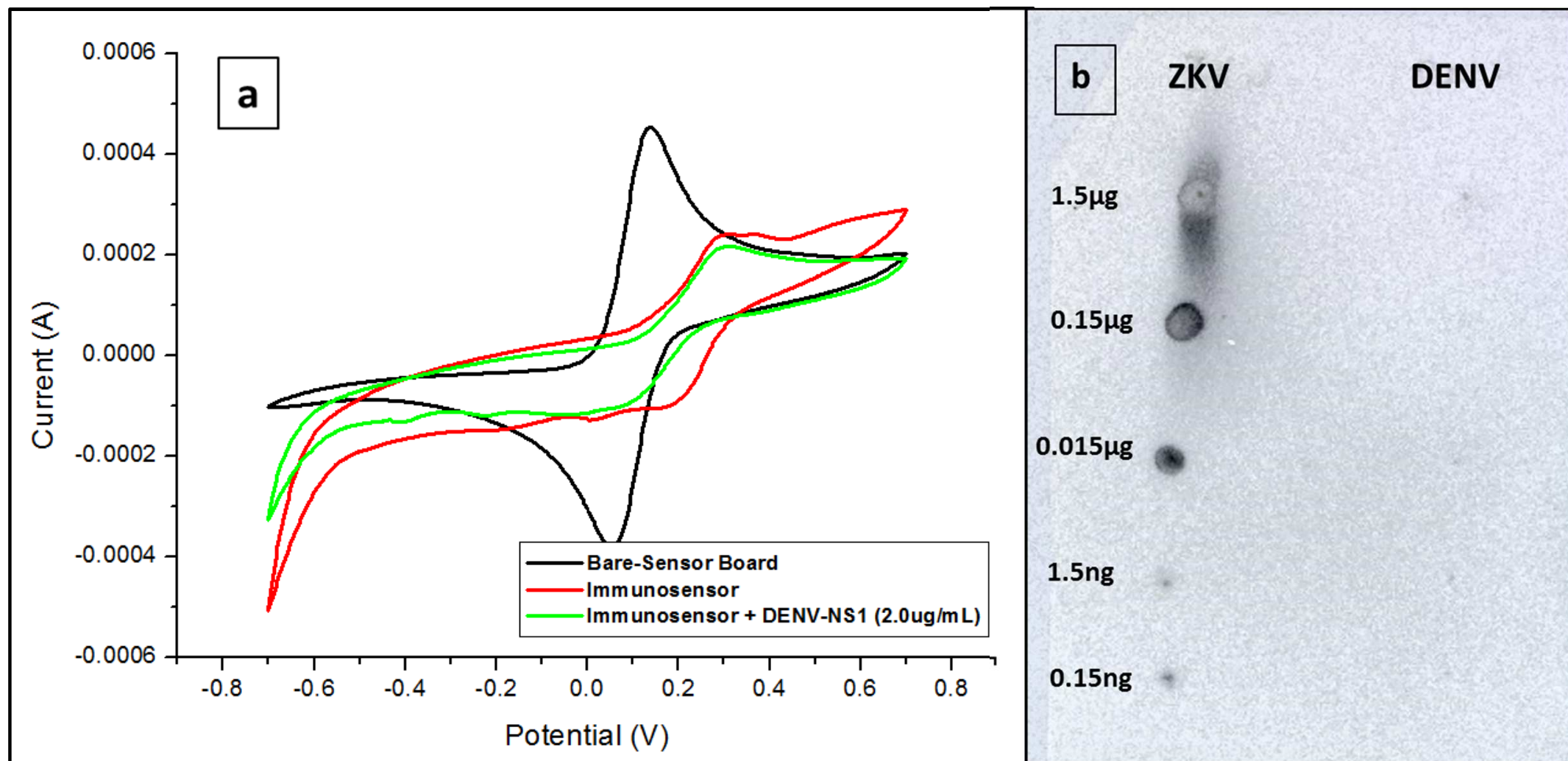
607

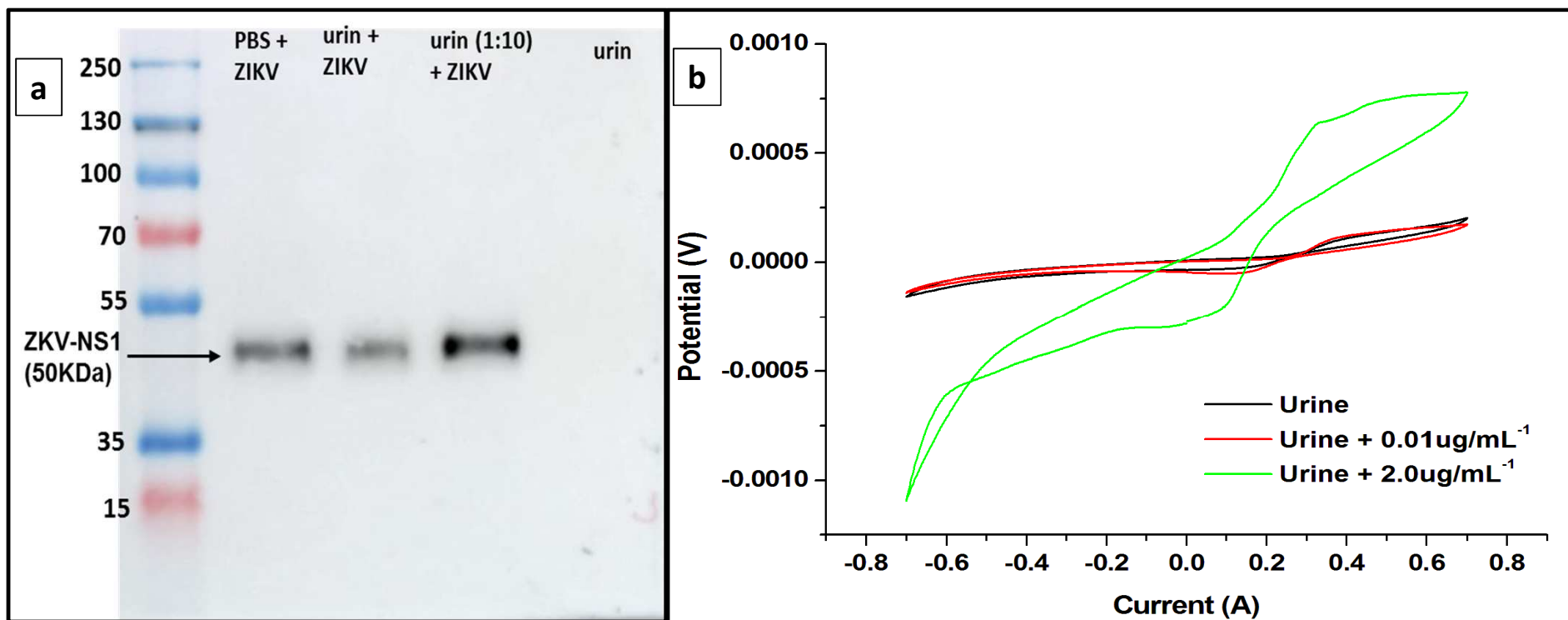












HIGHLIGHTS

- Effective approach in using printed circuit board sensors and ZnO nanorods on making low-cost, low limit of detection, high-speed, high specificity electrochemical immunosensor.
- Zika fever diagnosis using Zika nonstructural protein 1 antigen as a biomarker.
- Evidence of lack of cross-reaction of the immunosensor with DENV-1 NS1.
- Detection of ZKV-NS1 in urine samples
- Early detection of virus infection and noninvasive rapid test.